Nested grazing incidence optics for x ray detection*

Lin-Sen Li(李林森)[1,2,3], Peng-Fei Qiang(强鹏飞)[1,3,†], Li-Zhi Sheng(盛立志)[3], Yong-An Liu(刘永安)[1,3], Zhe Liu(刘哲)[3], Duo Liu(刘舵)[1,3], Bao-Sheng Zhao(赵宝升)[3], and Chun-Min Zhang(张淳民)[2]

[1] *University of Chinese Academy of Sciences, Beijing* 100049, *China*

[2] *School of Science, Xi'an Jiaotong University, Xi'an* 710119, *China*

[3] *State Key Laboratory of Transient Optics and Photonics, Xi'an Institute of Optics and Precision Mechanics, Xi'an* 710119, *China*

(Received 7 April 2017; revised manuscript received 3 July 2017; published online 20 August 2017)

Grazing incidence optics (GIO) is the most important compound in an x-ray detection system; it is used to concentrate the x-ray photons from outer space. A nested planar GIO for x-ray concentration is designed and developed by authors in this paper; planar segments are used as the reflection mirror instead of curved segments because of the simple process and low cost. After the complex assembling process with a special metal supporter, a final circle light spot of ϕ12 mm was obtained in the visible light testing experiment of GIO; the effective area of 1710.51 mm^2@1 keV and 530 mm^2@8 keV is obtained in the x-ray testing experiment with the GIO-SDD combination, which is supposed to be a concentrating detector in xray detection systems.

Keywords: x ray detection, grazing incidence optics, planar segments, concentrating detector

PACS: 07.85.Fv, 07.60.–j **DOI:** 10.1088/1674-1056/26/10/100703

1. Introduction

The x-ray grazing incidence optics (GIO), optical lenses, which could focus the x-ray incidence photons from a large grazing angle to a small point on the x-ray detector, and the large effective area may help the detection system find weak sources in outer space. According to the optical property, the grazing angle is always no more than 3°.[1]

In the past few years, kinds of GIO have been developed by NASA and ESA. The Chandra observatory,[2,3] previously known as the advanced x-ray astrophysics facility (AXAF), is a space observatory that was launched on STS-93 by NASA on July 23, 1999. Chandra is sensitive to x-ray sources 100 times fainter than any previous x-ray telescope, enabled by the high angular resolution (0.5″) of its four layer mirrors, which are made of microcrystalline glasses coated with iridium (Ir), where the film thickness is about 30 nm. The Chandra observatory is constructed based on the type of Wolter-I,[4,5] its focal length is 10.07 m and it works from 0.2 keV–10 keV. The European Space Agency's x-ray Multi-Mirror Mission[6,7] (XMM-Newton) was launched by Ariane 504 on December 10, 1999. XMM-Newton is ESA's second cornerstone of the Horizon 2000 Science Programme. It carries high throughput x-ray telescopes with an unprecedented effective area (4650 cm^2@1 keV), and an optical monitor, the first flown on an x-ray observatory. The large collecting area and ability to make long uninterrupted exposures provide highly sensitive observations. XMM-Newton is constructed based on the same type of Wolter-I as Chandra, and it has 58 mirrors integrated in the huge optical lenses. Suzaku[8–10] is Japan's fifth x-ray astronomy mission. It was developed at the Institute of Space and Astronautical Science of Japan's Aerospace Exploration Agency (ISAS/JAXA), Japan, in collaboration with U.S. (NASA/GSFC, MIT) and Japanese institutions, and was launched on July 10, 2005. Suzaku is the recovery mission for ASTRO-E, which did not achieve orbit during launch in February 2000. Suzaku is 2 orders lighter than Chandra and XMM-Newton, and the effective area is 440 cm^2@1.5 keV. Suzaku covers the energy range 0.2 keV–700 keV with three instruments: an x-ray micro-calorimeter (x-ray Spectrometer, or XRS), four x-ray CCDs (the x-ray Imaging Spectrometers, or XISs), and a hard x-ray detector, or HXD. However, the XRS prematurely lost all its liquid helium cryogen and is no longer operative. ASTRO-H[11,12] (also known as NEXT for New x-ray Telescope) is an x-ray astronomy satellite under construction by Japan's Aerospace Exploration Agency (JAXA) for studying extremely energetic processes in the universe. The space observatory is designed to extend the research conducted by the Advanced Satellite for Cosmology and Astrophysics (ASCA) by investigating the hard x-ray band above 10 keV. It was launched into a low Earth orbit in 2016 at an altitude of 550 km, but which failed after 3 days because of a tiny electrical mistake. NICER is a quasi Wolter telescope under construction by NASA which was launched on June 1, 2017; its purpose is to detect x-rays from Neutron star and verify x-ray communication.[13] NICER consists of 56 optical lenses with an overall effective area of 2000 cm^2@1 keV and

*Project supported by the National Natural Science Foundation of China (Grant No. 61471357) and the State Key Laboratory of Geo-Information Engineering Foundation (Grant No. SKLGIE2014-M-2-1).

†Corresponding author. E-mail: qiangpengfei@opt.ac.cn

© 2017 Chinese Physical Society and IOP Publishing Ltd

each one is 100 mm in diameter and 150 mm in height. The mirror in NICER is conical rather than parabolic or hyperbolic curve, because it is only used to count the photon numbers.

In this paper, the authors have developed a GIO with planar D263T glass coated with Ir film, there are 432 pieces of mirror integrating in the optics with different grazing incidence angles. An effective area of 1710.51 mm^2@1 keV is obtained with a silicon drift detector (SDD) integrating in the GIO detector.

2. Experimental section

2.1. Design of GIO

Focusing optics to date that have been engaged in the x-ray range are based on a very low angle, which is known as the grazing incidence angle in GIO. Regularly, when an incidence x-ray arrives at an object with a wide angle, it will penetrate the object because of the high energy of x-ray photons, which always used to be the principle of nondestructive testing and x-ray photography in medical treatments. When the incidence angle is narrow enough and the surface of the object the x-ray is encountering is smooth, x-ray photons would be reflected to the mirror direction at the same time as the visible light arrives on an interface with material that has a lower index of refraction. GIO mirrors have a low light harvesting area because of the existence of the grazing incidence angle, in order to obtain a higher light harvesting area, GIO was always designed as a nest structure, which consisted of certain layers of mirror with different incidence angles. The planar mirrors of GIO in this paper contain 24 layers of mirrors and each layer has a different incidence angle. The schematic picture is shown in Fig. 1. There are 24 concentric polygones in the planar GIO and they are different in diameter so as to integrate with each other perfectly.

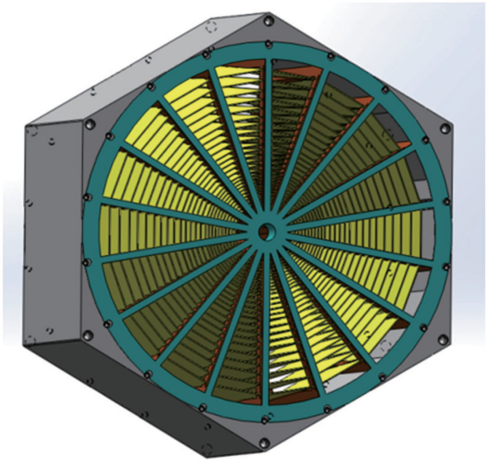


Fig. 1. (color online) Schematic diagram of planar GIO.

The design parameters of each polygone are as follows. The diameter of the largest polygones is 100 mm and detailed parameters are obtained

$$
\begin{aligned}
r_i &= f \cdot \tan 2\theta_i, \\
\sin\theta_i &= \frac{r_i(1-\varepsilon_i)}{L_0}, \\
h_i &= L_0 \sin\theta_i, \\
h_{i-1} &= d_i.
\end{aligned}
$$

In Fig. 2, r_i is the length between the center and vertex of each polygone in the incidence direction of planar GIO, θ_i is the grazing incidence angle of each layer, f is the focal length of planar GIO, $\varepsilon_i r_i$ is the length between the center and vertex of each polygone in the exiting direction of the planar GIO, h_i is the distance between two adjoining layers, and L_0 is the length of mirrors in the planar GIO.

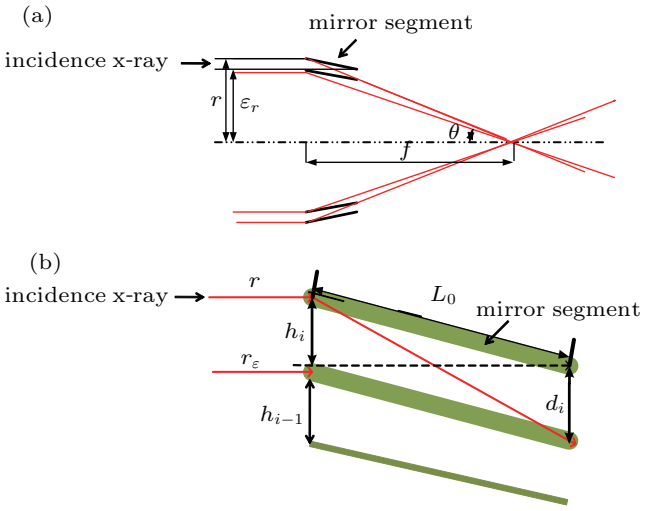


Fig. 2. (color online) Design progress of planar GIO. (a) The entire design progress of planar GIO, (b) the portion design process of planar GIO.

Table 1 lists the relevant parameters of GIO in the present study.

Table 1. Parameters of GIO.

Parameter	Value
Diameter of the outer mirror	100 mm
Focal length	1050 mm
Field of view	ϕ1.4°
Energy range	0.5 keV∼10 keV
Mirror length	150 mm
Number of layers	24
Diameter of the spot	12 mm

2.2. Development of the mirror segment

Mirror segments in planar GIO are developed with D263T glass because of the variety of advantages such as high strength, light weight, low coefficient of thermal expansion, and stability in physics and chemistry. However, the reflectivity of bare D263T glass is far from the demand of x-ray reflection, so in order to enhance the reflectivity of the mirror segment, Ir film is deposited on the D263T glass by electron

beam evaporation (EBE) technology. Figure 3 is the reflectivity of films prepared with different materials such as Ir, Ni, Au, Pt, Cr, and film of Ir to obtain the highest reflectance in the competition in the energy range below 2 keV, however, reflectance of all kinds of films in the range of 2 keV to 4 keV decrease sharply because of the high energy. So, Ir film is always chosen as the coating material in high energy range below 10-keV GIO.

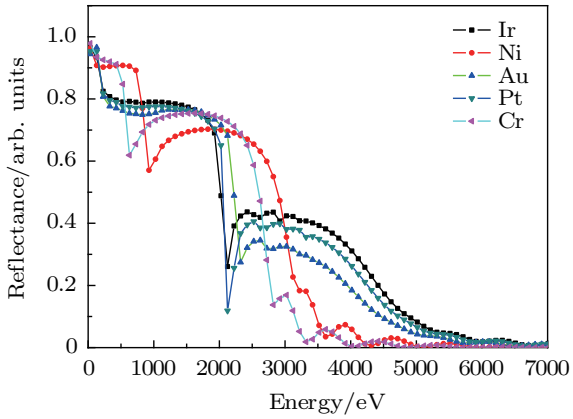


Fig. 3. (color online) The reflectivity of films prepared with different materials such as Ir, Ni, Au, Pt, and Cr.

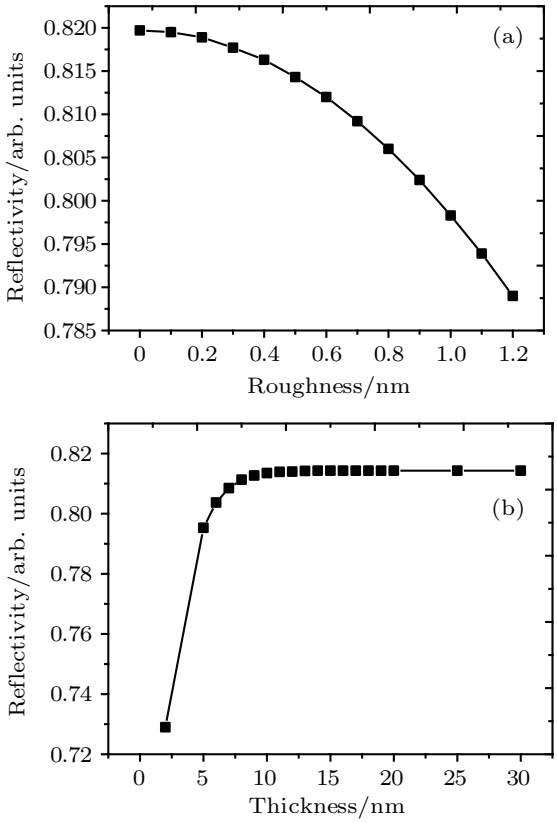


Fig. 4. Reflectivity @1 keV of Ir film with different roughnesses (a) and different thicknesses (b).

Then, the reflectivity of Ir film with different roughness and thickness is obtained in Fig. 4 (calculated by "http://henke.lbl.gov/optical_constants/"), the reflectivity decreases monotonously when the roughness of Ir film gets higher in Fig. 4(a), due to scattering occurring when photons arrive on the surface with defect, which is in the order of incidence light wavelength. Roughness is the most important factor influencing the performance of GIO, so the mirror segment should keep a lower roughness in order to obtain higher reflectivity. In Fig. 4(b), the reflectivity increases with the increase of film thickness and keeps stable after the value comes to 10 nm. So the authors choose 30-nm thickness of Ir film as the reflecting surface in GIO. Figure 5 shows the AFM graph of Ir film with different thicknesses on D263T glass; roughness values of 1.2 nm and 0.52 nm are obtained from Ir film with the thicknesses of 10 nm and 30 nm.

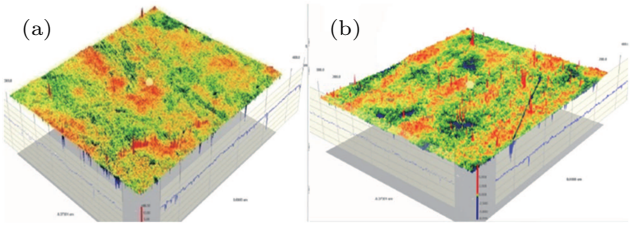


Fig. 5. (color online) AFM configuration of Ir film with the thickness of 10 nm (a) and 30 nm (b).

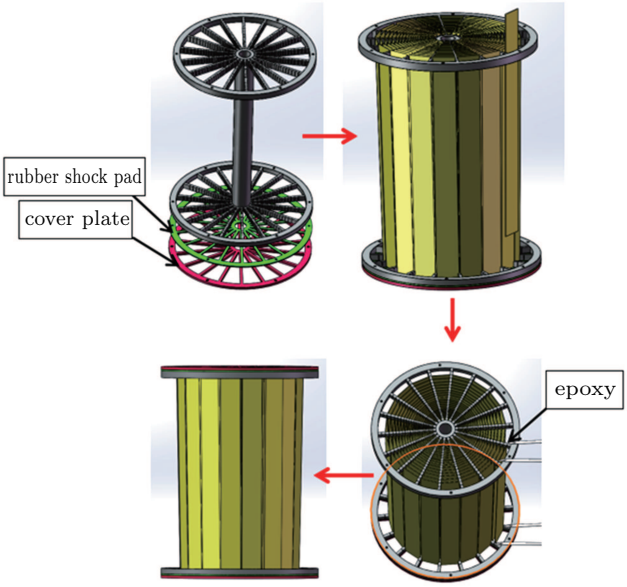


Fig. 6. (color online) The assembly process of the GIO.

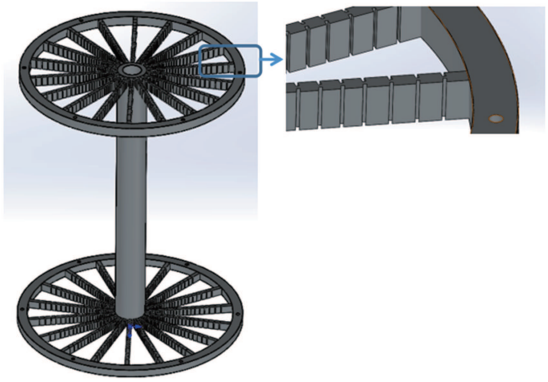


Fig. 7. (color online) The structure of the support frame.

Then, the mirrors are inserted into the grooves which are precisely manufactured on the bars of the support frame, and the mirrors are fixed with epoxy. Figure 6 shows the assembly process of the GIO. The structure of the support frame is shown in Fig. 7.

2.3. Testing

Mirror segments were assembled into various concentric polygones with a metal supporter which was specially designed; all segments are assembled on the designated position as shown in Figs. 8(a) and 8(b). When all the segments were assembled together, a special metal shielding was used to be a cover to the fragile glass component (Fig. 8(c)).

The x-ray testing progress was developed in a vacuum pipeline as shown in Figs. 8(d) and 8(e). Figure 8(d) is the software of the SDD detector and it is used to count the x-ray photon number in the vacuum pipeline. Figure 8(e) is a grid-control x-ray source developed by Zhao's team in the Xi'an Institute of Optics and Precision Mechanics,[14–16] which is used to produce kinds of periodic signals for simulating pulsars from the distance of light years.

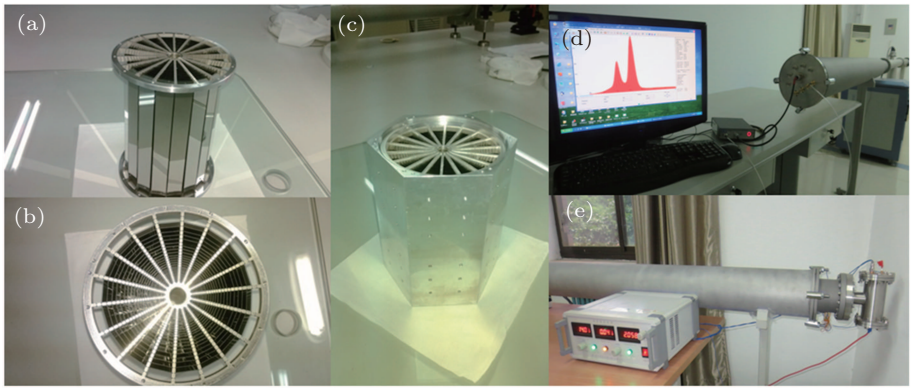


Fig. 8. (color online) (a) and (b) The assembling process planar GIO; (c) the assembled planar GIO; (d) and (e) the ground simulation system of x-ray pulsar navigation technology in Xi'an Institute of Optics and Precision Mechanics.

3. Result and discussion

Figure 9 is the focus spot of the x-ray transporting through the planar GIO in the distance of 1050 mm, which is the designed focal length of planar GIO, when collimated light comes in from the entrance (larger diameter direction) of the GIO, grazing incidence occurs and a circle light spot is obtained in the x-ray display integrated by the micro channel plate detector, and the diameter of the spot is 12 mm (W90) from the image scale. The reason for the large focus spot is that we use the planar mirror segment to assemble the GIO instead of a curved mirror segment; the advantage of a planar mirror segment is that the glass coated with Ir film never needs to be slumped at a high temperature, in which progress much more middle frequency would generate on the surface of D263T glass, and slumping technology is too complex to complete in a short time.

Figure 10 is the result of the effective area testing experiment in the wavelength of x-ray that is produced by the grid-control x-ray source in the Xi'an Institute of Optics and Precision Mechanics. When collimated x-ray comes in from the entrance of the GIO, grazing incidence occurs and an invisible x-ray circle light spot is obtained in the SDD detector. The red areas in Fig. 8 are the photon number detected by SDD without planar GIO. Comparing with the colorless areas which are the photon number detected by SDD with planar GIO, the result without GIO decreases heavily in every range of x-ray, which is due to the concentration effect of the planar GIO. The effective area of 1710.51 mm^2@1 keV is obtained in Fig. 8(a) under the condition of 5 keV (anode voltage) x-ray source, and the entrance area of planar GIO is 5304 mm^2, however, the concentration effect would be weak with the increasing of anode voltage of the x-ray source.

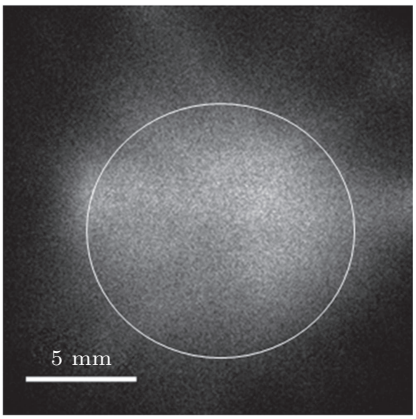


Fig. 9. The focal spot of planar GIO in x-ray testing experiment.

Figure 11 is the concentration efficiency of planar GIO in the range 0 keV–8 keV. The concentration efficiency is the ratio of effective area and entrance area in GIO. A descending trend is obtained with the energy increasing in x-ray wavelength, which shows that a higher energy x-ray needs a lower grazing incidence angle to realize total reflection. The reflection of high energy x-ray is supposed to be lower than that of low energy x-ray, and an effective area of 530 mm^2@8 keV is obtained in the x-ray testing experiment.

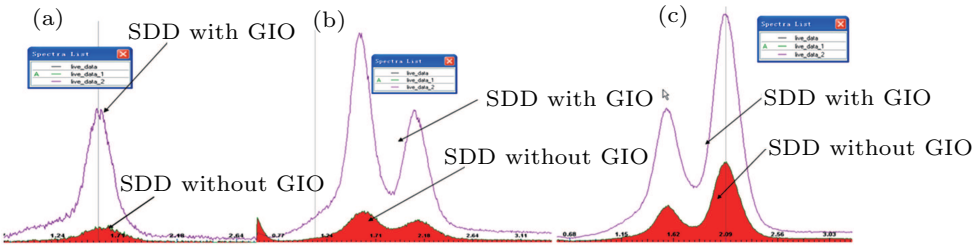


Fig. 10. (color online) The testing experiment of planar GIO in the wavelength of x-ray, the anode voltage of x-ray source is 5 kV (a), 10 kV (b), and 15 kV (c).

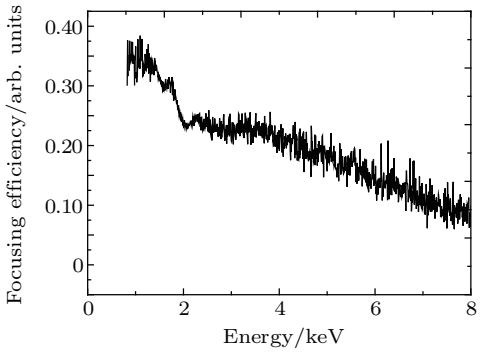


Fig. 11. Concentration efficiency of planar GIO.

4. Conclusion

In this paper, an easy-manufactured planar GIO for x-ray concentration is designed and developed by authors, planar D263T glasses coated with Ir film are used as the reflection mirror instead of curved segments because of the simple process and low cost. A metal supporter is specially designed and used for assembling mirrors together. Finally, the planar GIO is tested in the ground simulation system of Pulsar navigation in the Xi'an Institute of Optics and Precision Mechanics. A circle light spot of ϕ12 mm was obtained in visible light testing experiment, and the effective area of 1710.51 mm^2@1 keV and 530 mm^2@8 keV is obtained in x-ray testing experiment with the GIO-SDD combination.

Acknowledgment

This research was supported by the West Light Foundation of the Chinese Academy of Sciences.

References

[1] Peng S Q, Liu Z G, Sun T X, Wang K, Yi L T, Yang K, Chen M and Wang J B 2016 *Chin. Phys. B* **25** 024102

[2] Brinkman A C 1991 *Adv. Space Res.* **11** 231

[3] Weisskopf M C and Speybroeck L V 1986 *Opt. Photon. News* **7** 16

[4] Feldman C and Willingale R P 2012 *Adaptive X-Ray Optics II15* **8503** 39

[5] Culhane J R, Catura K, Pounds P, Korte D, Franks A, Garmire G, FabianA, Margon B and Natuurwetenschappen F 1981 *Space Sci. Rev.* **30** 581

[6] Truemper J and Tananbaum H 2003 *X-Ray and Gamma-Ray Telescopes and Instruments for Astronomy* **4851** 140

[7] Watson M G, Schroder A C, Fyfe D, *et al.* 2009 *Astronomy & Astrophysics* **493** 339

[8] Nakagawa Y T, Mihara A, Yoshida K, Yamaoka S, Sugita T, Murakami D, Yonetoku M, Suzuki M, Nakajima M, Tashiro and Nakazawa K 2008 *Publica-tions of the Astronomical Society of Japan* **61** S387

[9] Bamba A G, Puehlhofer F, Acero D, Klochkov W, Tian R, Yamazaki Z, Li D, Horns K, Kosack and Komin N 2012 *The Astrophysical Journal* **761** 80

[10] Ueno M R, Sato J, Kataoka A, Bamba I, Harrus J, Hughes C, Kilbourne K, Koyama M, Kokubun H, Nakajima M, Ozaki R, Petre T, Takahashi T, Tanaka H, Tomida and Yamaguchi H 2007 *Prog. Theor. Phys. Supplement* **59** 897

[11] Takahashi T, Mitsuda K and Kelley R 2004 *Bull. Am. Astron. Soc.* **36** 925

[12] Robinson D, Okajima T, Serlemitsos P and Soong Y 2012 *Aerospace Conference* **186** 1

[13] Sheng L Z, Zhao B S and Liu Y A 2014 *SPIE Advances in X-Ray/EUV Optics and Components IX5*, September, **920** 716

[14] Hu H J, Zhao B S, Sheng L Z and Yan Q R 2011 *Acta Phys. Sin.* **60** 29701 (in Chinese)

[15] Ma X F, Zhao B S, Sheng LZ, Liu Y A, Liu D and Deng N Q 2014 *Acta Phys. Sin.* **63** 160701 (in Chinese)

[16] Dai J F Zhao B S and Sheng L Z 2015 *Acta Phys. Sin.* **64** 149701 (in Chinese)